

Intensities of the γ -ray emissions following the ^{111}Sn decay determined via photonuclear reaction yield measurements

A. Chekhovska^{a,b}, Ye. Skakun^a, I. Semisalov^a, S. Karpus^a and V. Kasilov^a

^aNational Scientific Center Kharkiv Institute of Physics and Technology, 1 Akademicheskaya St., Kharkiv, 61108, Ukraine

^bV. N. Karazin Kharkiv National University, 4 Svobody Sq., Kharkiv, 61022, Ukraine

ARTICLE INFO

Keywords:
 Radioactive decay
 Photonuclear reactions
 Bremsstrahlung
 γ -Ray emissions

ABSTRACT

The intensities of the ten strongest γ -ray transitions following the ^{111}Sn ($T_{1/2}=35.3$ m) decay have been determined via comparison of the two sets of the experimental photonucleon reaction yields driven using the traditional activation equation and the activation equation for the genetically coupled radioactive nuclei. The found absolute intensities of the γ -ray transitions in question were happened to be noticeably different from the currently recommended values.

1. Introduction

Nucleus decay data are important for both nuclear spectroscopy theories and experimental techniques determining nuclear reaction cross sections or yields by means of residual activity measurements. The tin-111 (^{111}Sn) nucleus decaying by ($\epsilon + \beta^+$)-process with the half-life of 35.3 m populates a large array of excited levels of the indium-111 (^{111}In) daughter nuclide among which there is an isomeric state with the excitation energy 537.2 keV and the half-life $T_{1/2}^m = 7.7$ m (Fig. 1). The ground state of the ^{111}In nuclide ($T_{1/2}^g = 2.80$ d) decays to the stable ^{111}Cd one following the strong γ -ray transitions of 171.2 keV and 245.3 keV. The last evaluated decay data for the A=111 nuclear mass were recommended by publication [1] and involved to NuDat 2.8 base [2]. Meanwhile the intensity values of the γ -ray transitions between the ^{111}In excited levels following the ^{111}Sn decay are based on the relatively old experimental measurements, mostly performed at the 1970-1980s (see references of [1]), and taken with detectors of relatively low efficiencies and poor resolutions compared with the current γ -ray spectrometry techniques.

A large quantity of experimental measurements of activation cross sections and yields of different nuclear reactions induced by various incident particles, which lead to the formation of the ^{111}Sn nuclide, have been carried out for basic and applied purposes to date [3]. The correct values of the γ -ray emissions following the residual nuclei are needed for the correct determination of the nuclear reaction cross sections or yields using a γ -ray spectrometry activation technique. We have met this problem determining the bremsstrahlung activation yields of the near-threshold photonuclear reactions on the ^{112}Sn nuclide as a target which are partly of interest as input data for studying the γ -scenario of the stellar nucleosynthesis of the so-called p -nuclei [4, 5].

2. Experimental procedure and analysis

2.1. General notes

The ^{111}Sn radioisotope was produced by the $^{112}Sn(\gamma, n)^{111}Sn$ photonuclear reaction at the 30 MeV electron linear accelerator located at the National Scientific Center Kharkiv Institute of Physics and Technology (NSC KIPT). The electron beam of ~ 10 μ A current and 15 MeV and less energies impacted to the 100 μ m tantalum foil to be converted to a bremsstrahlung photon flux irradiating the investigated target placed along the electron beam axis while non-converted electrons were deflected with a permanent magnet. Four self-supporting tin metallic foils having the square shape with side 18 mm and total weighing 77 mg enriched with the ^{112}Sn isotope to 80% level were used as the unified target. At every irradiation the gold foil of 20 mm in diameter weighing 120 mg was placed with the studied tin target in the close geometry in order to use the $^{197}Au(\gamma, n)^{196}Au$ reaction as the standard one to determine the

*Corresponding authors

✉ chekhovska@kipt.kharkov.ua (A. Chekhovska); skakun@kipt.kharkov.ua (Ye. Skakun); semisalov@kipt.kharkov.ua (I. Semisalov); karpus@kipt.kharkov.ua (S. Karpus); kasilov@kipt.kharkov.ua (V. Kasilov)
 ORCID(s):

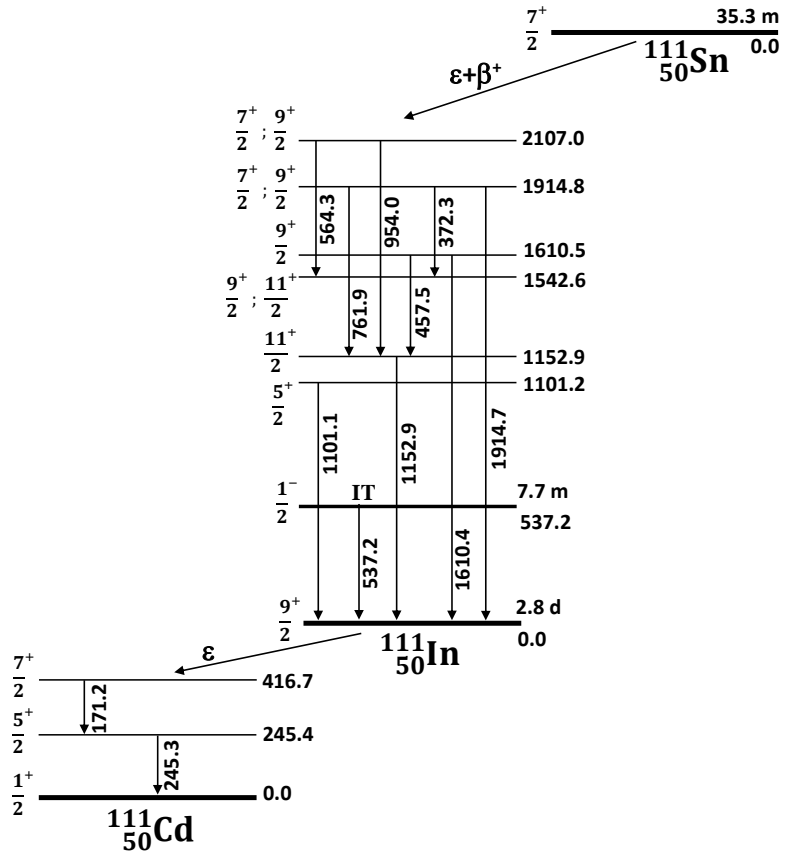


Figure 1: Simplified scheme of the $^{111}\text{Sn} \rightarrow {}^{111m,g}\text{In} \rightarrow {}^{111}\text{Cd}$ radioactive chain.

bremsstrahlung flux. The cross sections of the last reaction were earlier measured and evaluated by several experimental teams [6, 7, 8, 9] in the giant resonance region the results of which are consistent each with other well and the ^{196}Au residual radioactive decay has the very suitable properties [2] for its activity measurement. The ionization chamber placed along the beam axis was monitoring the photon flux crossing both targets during irradiations. Several exposures of such the combined target (the target sandwich) were carried out over a range of bremsstrahlung endpoint energies between the threshold of the $^{112}\text{Sn}(\gamma, n)^{111}\text{Sn}$ reaction (10.79 MeV) and 15 MeV to obtain the energy dependence of the photoactivation yield.

After each irradiation lasting usually ~ 100 m the targets were delivered to a low-background room far from the accelerator as soon as possible in order to begin to measure the energy spectra of γ -rays following the radioactive decay of the ^{111}Sn and its daughter ^{111}In using a coaxial Canberra High Purity Germanium detector with relative efficiency of 30% in comparison to the efficiency of (3 in. $\tilde{\text{A}}$ 3 in.) $\text{NaI}(Tl)$ -detector and 1.8 keV resolution for the 1332 keV γ -line of the ^{60}Co isotope source. To reduce ambient radioactivity the detector was contained in a lead shield, with walls 12 cm in depth and degraders of 3 mm Cd and 5 mm Cu line the inside of the shield to reduce the interference of the Pb fluorescence X-rays. The γ -ray spectra of the ^{196}Au ($T_{1/2} = 6.16$ d [2]) residual nucleus of the standard reaction were measured secondarily. The irradiated targets were mounted along the vertical axis of the spectrometer on several sample-to-detector distances between 5 and 10 cm. The measurements of the detector full-energy-peak efficiency were performed at the (50-1500) keV γ -ray energy region using ^{22}Na , ^{60}Co , ^{133}Ba , ^{137}Cs , ^{152}Eu , ^{226}Ra , and ^{241}Am calibrated point sources. Fig. 2 shows the energy dependences of the detector efficiency for the two distances between the source and crystal end-cup.

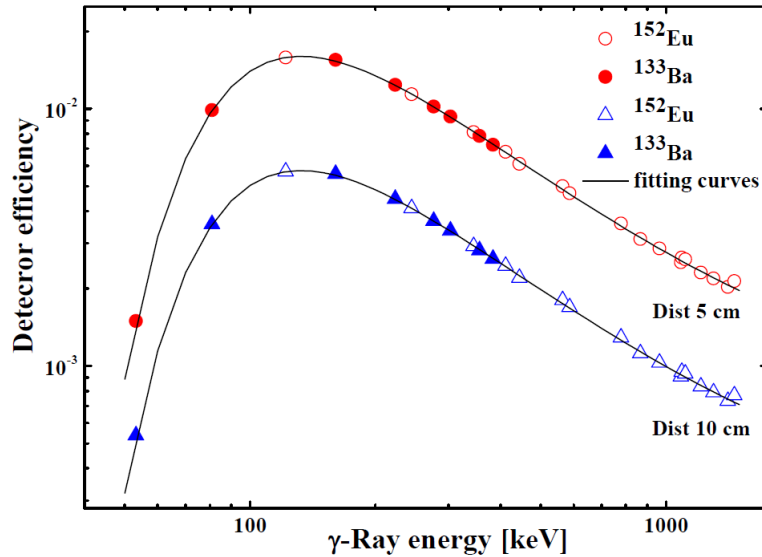


Figure 2: The full-energy peak detection efficiency curves of the HPGe γ -ray spectrometer for sample-to-end-cap distances 5 and 10 cm.

2.2. Activity measurements

The two typical γ -ray spectra of the ^{112}Sn target irradiated with 15 MeV bremsstrahlung are shown in Fig. 3. A shorter-live fraction of the induced radioactivity is given in the upper panel, a longer-live one in the lower one. The arrows of the upper panel indicate the 10 strongest gamma-ray transitions in the ^{111}In nucleus following the ^{111}Sn decay. The energy of each transition is indicated in kiloelectron-volt units above the arrow.

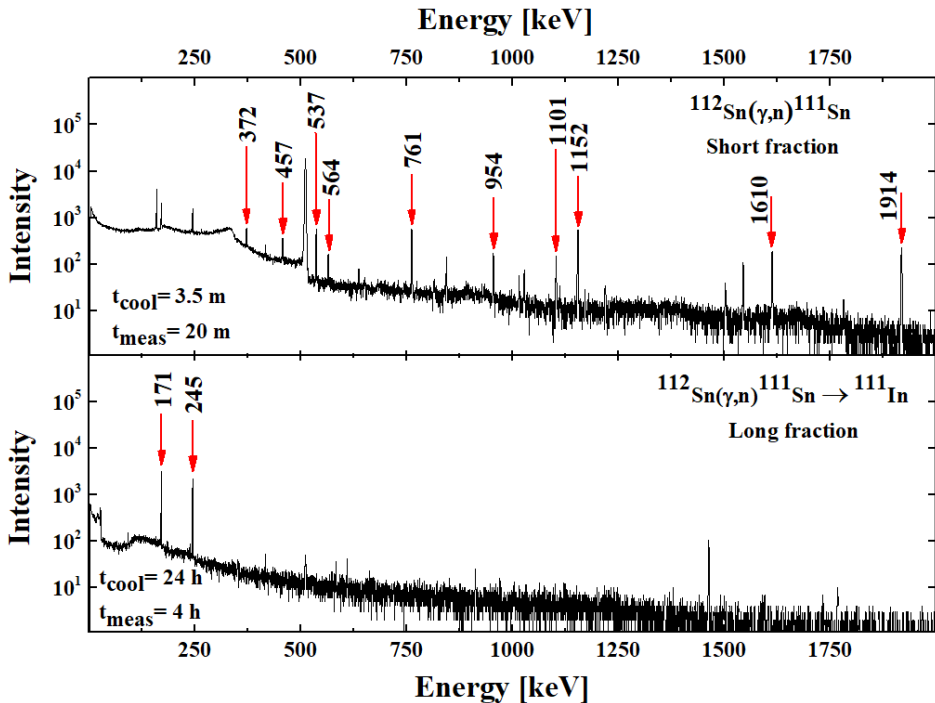
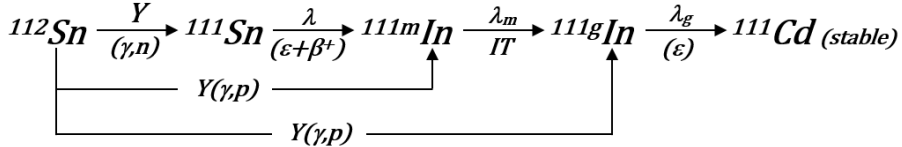


Figure 3: Short (upper panel) and long (lower panel) fractions of the typical γ -ray spectrum measured after irradiation of the ^{112}Sn target with 15 MeV bremsstrahlung.

The γ -ray spectrum measured one day later irradiation (the lower panel of Fig. 3), except weak background, contains only 2 strong peaks (171 keV and 245 keV, indicated with arrows), which are correspond to the γ -rays following the decay of the ^{111}In nucleus ($T_{1/2}^g = 2.80$ d) being the daughter of the ^{111}Sn nucleus (see Fig. 1) and on the other side can be additionally produced via the $^{112}\text{Sn}(\gamma, \text{p})^{111m+g}\text{In}$ reaction (the 7.55 MeV threshold) in appliance with the scheme:



The energies and intensities of the mentioned γ -ray transitions of the $^{111}\text{Sn} \rightarrow ^{111}\text{In} \rightarrow ^{111}\text{Cd}$ radioactive chain borrowed from NuDat 2.8 base [2] are presented in Table. 1.

Table 1

Energies and intensities of the γ -ray transitions following the ^{111}Sn , ^{111m}In , and ^{111g}In decays [2]

E_γ [keV]	I_γ [%]
$^{111}\text{Sn} \rightarrow ^{111}\text{In}$	
372.3	0.42 (7)
457.5	0.38 (6)
537.2	0.25 (4)
564.3	0.30 (5)
761.9	1.48 (23)
954.0	0.51 (8)
1101.1	0.64 (11)
1152.9	2.65 (40)
1610.4	1.31 (20)
1914.7	2.0 (3)
$^{111m}\text{In} \rightarrow ^{111g}\text{In}$	
537.2	87.2 (5)
$^{111g}\text{In} \rightarrow ^{111}\text{Cd}$	
171.2	90.7 (9)
245.3	94.1 (10)

2.3. Experimental data analysis

The radioactive decay curves derived analyzing the two most intense γ -ray transitions (761.9 and 1152.9 keV) of the ^{111}In daughter nucleus are depicted in Fig. 4. The half-life values (indicated in the plot) of the ^{111}Sn radionuclide determined from the time dependencies of the intensities of these two γ -lines are in good agreement with the NuDat 2.8 base value 35.3 (6) m [2]. The remaining gamma lines following the ^{111}Sn decay obey the same consistent pattern of exponential decay.

The bremsstrahlung activation yield Y of the $^{112}\text{Sn}(\gamma, \text{n})^{111}\text{Sn}$ reaction can be determined solving the traditional activation equation (1)

$$\frac{S_\gamma}{\varepsilon \cdot \text{Br} \cdot n \cdot \phi} = \frac{Y}{\lambda} \cdot (1 - e^{-\lambda t_1}) \cdot e^{-\lambda t_2} \cdot (1 - e^{-\lambda t_3}) \quad (1)$$

in which S_γ is the experimental area of any γ -ray peak of the ^{111}Sn decay, ε the full-energy peak detection efficiency, $\text{Br} = I_\gamma / 100$ branching coefficient of the same γ -ray transition, n the number of nuclei in the target being irradiated, ϕ the flux of the bremsstrahlung photons covering the target, λ radioactive decay constant, t_1 , t_2 , and t_3 the irradiation, cooling and measurement times of the target activity respectively.

De-excitation of the ^{111}In states (including the ^{111m}In isomer) populated by the decay of ^{111}Sn leads to the ^{111}In ground state. The experimental areas S_γ of the 171.2 keV and 245.3 keV γ -ray peaks of the ^{111g}In decay at the

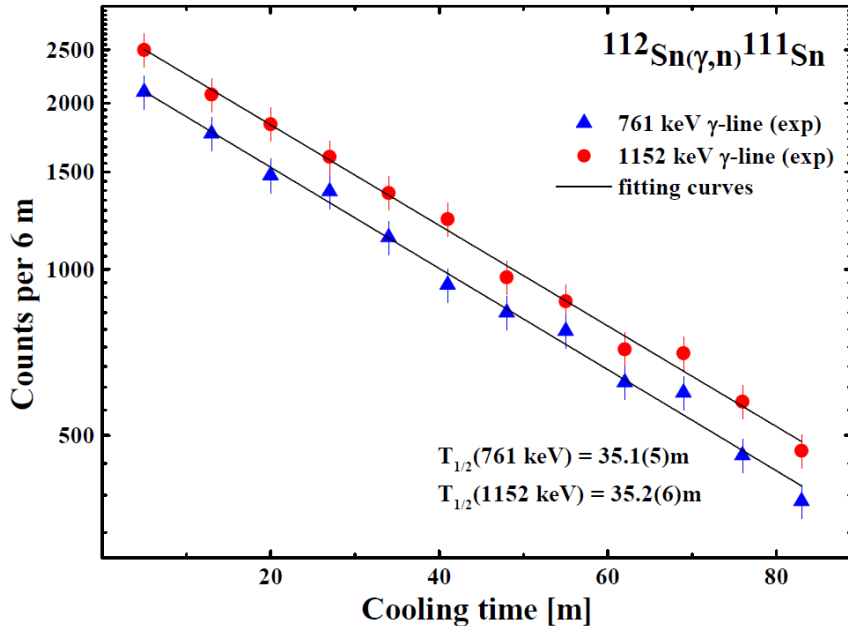


Figure 4: Decay curves of the ^{111}Sn radioactive nucleus constructed from the 761 keV and 1152 keV γ -line intensities.

t_2 cooling time much more 7.7 m (the ^{111m}In isomer half-life) obey the equation (2) [10] for genetically-coupled radioactive nuclides

$$\frac{S_\gamma}{\varepsilon \cdot \text{Br} \cdot n \cdot \phi} = Y_p \cdot \frac{\lambda_p \cdot \lambda_d}{\lambda_d - \lambda_p} \cdot \left[\frac{1 - e^{-\lambda_p t_1}}{\lambda_p^2} \cdot e^{-\lambda_p t_2} \cdot (1 - e^{-\lambda_p t_3}) - \frac{1 - e^{-\lambda_d t_1}}{\lambda_d^2} \cdot e^{-\lambda_d t_2} \cdot (1 - e^{-\lambda_d t_3}) \right] + Y_d \frac{1 - e^{-\lambda_d t_1}}{\lambda_d} \cdot e^{-\lambda_d t_2} \cdot (1 - e^{-\lambda_d t_3}) \quad (2)$$

where in our case Y_p and Y_d are the yields of the parent (^{111}Sn) and daughter (^{111}In) nuclei, λ_p and λ_d the decay constants of the parent and daughter nuclei respectively.

The curves of the ^{111}In nucleus accumulation and decay plotted according to the experimental γ -line intensities 171.2 keV and 245.3 keV, measured after the end of irradiation of the tin target, are shown in Fig. 5. These time dependences obey equation (2) and their forms are due to the differences of the half-lives of the parent and daughter members of the radioactive chain and the values of the yields (Y_p and Y_d in the equation (2)) of the $^{112}\text{Sn}(\gamma, \text{n})^{111}\text{Sn}$ and $^{112}\text{Sn}(\gamma, \text{p})^{111}\text{In}$ reactions respectively. The growing pieces of the ^{111}In activity curves at the left part of Fig. 5 are explained by the feeding of the longer-living nucleus by the shorter-living one decay. Fitting the equation (2) for genetically-coupled activities by least squares method we were able to determine the values of the both yields and obtained an unexpected result: the values of Y_p (i. e. of the $^{112}\text{Sn}(\gamma, \text{n})^{111}\text{Sn}$) reaction turned out to be noticeably less than those determined using the traditional activation equation (1). Both data sets for different bremsstrahlung energies are shown in Fig. 6. The decay features of the long-lived ^{111}In nucleus are investigated quite well to date and the only reason for this observation may be large uncertainties of the experimental values of the γ -ray emission values of the radiation transitions following the ^{111}Sn isotope decay.

The circles of Fig. 6 represent the experimental weighted average values of the photonuclear $^{112}\text{Sn}(\gamma, \text{n})^{111}\text{Sn}$ reaction yields calculated applying the traditional activation equation (1) and the current [2] γ -ray emission values of the 10 strongest γ -ray transitions of the $^{111}\text{Sn} \rightarrow ^{111}\text{In}$ decay. The set of the triangles was obtained applying equation (2) for genetically coupled activities and the database [2] emission values of the 171.2 keV and 245.3 keV γ -rays of the $^{111}\text{In} \rightarrow ^{111}\text{Cd}$ decay.

The numerous measurements and analysis of the decay γ -ray energy spectra at different bremsstrahlung energies and cooling times of the irradiated target enable us to recalculate the new values of the γ -ray emission values for the 10 strongest radiation transitions following the ^{111}Sn nucleus radioactive decay. The intensities of the 9 transitions, excluding the 537.2 keV one, were happened to be lower those of NuDat 2.8 base [2] at the average factor of 1.64

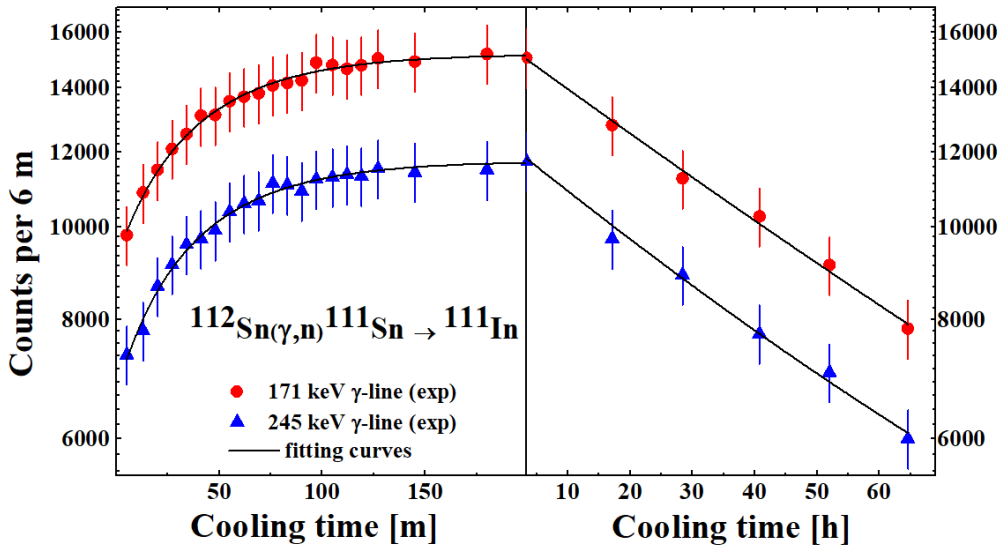


Figure 5: Accumulation and decay curves of the ^{111}In isotope nuclide.

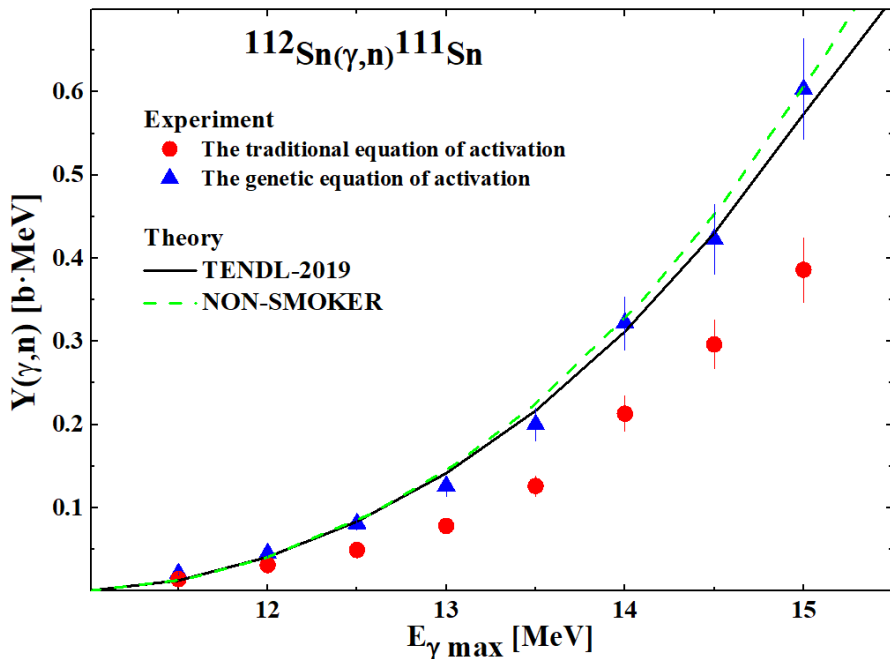


Figure 6: The $^{112}\text{Sn}(\gamma, n)^{111}\text{Sn}$ reaction yields determined using the traditional activation equation (circles) and equation for genetically coupled activities (triangles).

(0.10). The 537.2 keV γ -ray intensity recalculating taking into account different contributions of the (γ, n) and (γ, p) reactions is lower at the factor of 1.92 (0.16).

In addition the solid and dashed curves in Fig. 6 represent the integral bremsstrahlung yields of the $^{112}\text{Sn}(\gamma, n)^{111}\text{Sn}$ reaction calculated from the cross sections predicted by the statistical theory of nuclear reactions implemented in the NON-SMOKER computer code [11] and TENDL-2019 data library [12] respectively. Further interpretation of the $^{112}\text{Sn}(\gamma, n)^{111}\text{Sn}$ and $^{112}\text{Sn}(\gamma, p)^{111m,g}\text{In}$ activation yields are currently underway.

3. Conclusions

So we can present updated values of the intensities of the 10 γ -ray transitions following the ^{111}Sn radioactive decay. They are presented in the right column of Table 2.

Table 2

New intensities of the ^{111}In γ -ray transitions following the $(\epsilon + \beta^+)$ -decay of the ^{111}Sn nucleus.

E_γ [keV]	I_γ [%]	
	NuDat	New data
372.3	0.42 ± 0.07	0.26 ± 0.05
457.56	0.38 ± 0.06	0.23 ± 0.04
537.2	0.25 ± 0.04	0.13 ± 0.03
564.34	0.30 ± 0.05	0.18 ± 0.04
761.97	1.48 ± 0.23	0.90 ± 0.08
954.05	0.51 ± 0.08	0.31 ± 0.05
1101.18	0.64 ± 0.11	0.39 ± 0.0
1152.98	2.7	1.65 ± 0.10
1610.47	1.31 ± 0.20	0.80 ± 0.09
1914.70	2.0 ± 0.03	1.21 ± 0.12

The new intensity values of the γ -ray emissions following the ^{111}Sn nucleus decay will be interest for both nuclear spectroscopy theories and correct calculations of activation cross sections and yields of those nuclear reactions where the ^{111}Sn radioactive nuclide is a residual one. The numerous relevant data presented in the EXFOR database have to be revised.

References

- [1] J. Blachot, Nuclear Data Sheets for A = 111, Nuclear Data Sheets 110 (2009) 1239 - 1407. [doi:10.1016/j.nds.2009.04.002](https://doi.org/10.1016/j.nds.2009.04.002).
- [2] <https://www.nndc.bnl.gov/nudat2/>.
- [3] <https://www.nndc.bnl.gov/exfor/>.
- [4] T. Rauscher, N. Dauphas, I. Dillmann, C. Fröhlich, Z. Fülop, G. Gyürky, Constraining the astrophysical origin of the p-nuclei through nuclear physics and meteoritic data, Reports on Progress in Physics 76 (6) (2013) 066201. [doi:10.1088/0034-4885/76/6/066201](https://doi.org/10.1088/0034-4885/76/6/066201).
- [5] T. Rauscher, Photonuclear reactions in astrophysics, Nuclear Physics News 28 (3) (2018) 12 - 15. [doi:10.1080/10619127.2018.1463016](https://doi.org/10.1080/10619127.2018.1463016).
- [6] O. Itoh, H. Utsunomiya, H. Akimune, T. Kondo, M. Kamata, T. Yamagata, H. Toyokawa, H. Harada, F. Kitatani, S. Goko, C. Nair, Y.W. Lui, Photoneutron Cross Sections for Au Revisited: Measurements with Laser Compton Scattering γ -Rays and Data Reduction by a Least-Squares Method, Journal of Nuclear Science and Technology 48 (5) (2011) 834 - 840. [doi:10.1080/18811248.2011.9711766](https://doi.org/10.1080/18811248.2011.9711766).
- [7] V. V. Varlamov, B. S. Ishkhanov, V. N. Orlin, S. Y. Troshchiev, New Data for $^{197}Au(\gamma, nX)$ and $^{197}Au(\gamma, 2nX)$ Reaction Cross Sections, Bulletin of the Russian Academy of Sciences: Physics 74 (2010) 842 - 849. [doi:10.3103/S1062873810060237](https://doi.org/10.3103/S1062873810060237).
- [8] C. Nair, M. Erhard, A. R. Junghans, D. Bemmerer, R. Beyer, E. Grosse, J. Klug, K. Kosev, G. Rusev, K. D. Schilling, et al., Photoactivation experiment on ^{197}Au and its implications for the dipole strength in heavy nuclei, Physical Review C 78 (5) (2008) 055802. [doi:10.1103/physrevc.78.055802](https://doi.org/10.1103/physrevc.78.055802).
- [9] C. Plaisir, F. Hannachi, F. Gobet, M. Tarisien, m.-m. Aleonard, V. Meot, G. Gosselin, P. Morel, B. Morillon, Measurement of the $^{85}Rb(\gamma, n)^{84m}Rb$ cross-section in the energy range 10-19 MeV with bremsstrahlung photons, The European Physical Journal A 48 (2012) 68 - 72. [doi:10.1140/epja/i2012-12068-7](https://doi.org/10.1140/epja/i2012-12068-7).
- [10] G. Friedlander, J. W. Kennedy, J. M. Miller, Book, Nuclear and radiochemistry 14 (John Wiley and Sons, Inc., New York) (1981).
- [11] T. Rauscher, F.-K. Thielemann, Astrophysical Reaction Rates From Statistical Model Calculations, Atomic Data and Nuclear Data Tables 75 (1-2) (2000) 1 - 351. [doi:10.1006/adnd.2000.0834](https://doi.org/10.1006/adnd.2000.0834).
- [12] https://tendl.web.psi.ch/tendl_2019/tendl2019.html.